

## Optical properties of SrTiO<sub>3</sub> on silicon(100)

Yao Tian, Carolina Adamo, Darrell G. Schlom, and Kenneth S. Burch

Citation: *Appl. Phys. Lett.* **102**, 041906 (2013); doi: 10.1063/1.4789752

View online: <http://dx.doi.org/10.1063/1.4789752>

View Table of Contents: <http://apl.aip.org/resource/1/APPLAB/v102/i4>

Published by the American Institute of Physics.

### Related Articles

X-ray diffraction and extended X-ray absorption fine structure study of epitaxial mixed ternary bixbyite Pr<sub>x</sub>Y<sub>2-x</sub>O<sub>3</sub> (x=0–2) films on Si (111)

*J. Appl. Phys.* **113**, 043504 (2013)

Photocarrier generation in Cu<sub>x</sub>O thin films deposited by radio frequency sputtering

*Appl. Phys. Lett.* **102**, 032101 (2013)

Experimental and theoretical investigation of the electronic structure of Cu<sub>2</sub>O and CuO thin films on Cu(110) using x-ray photoelectron and absorption spectroscopy

*J. Chem. Phys.* **138**, 024704 (2013)

Optical band gap of NpO<sub>2</sub> and PuO<sub>2</sub> from optical absorbance of epitaxial films

*J. Appl. Phys.* **113**, 013515 (2013)

Crystal field splitting and optical bandgap of hexagonal LuFeO<sub>3</sub> films

*Appl. Phys. Lett.* **101**, 241907 (2012)

### Additional information on *Appl. Phys. Lett.*

Journal Homepage: <http://apl.aip.org/>

Journal Information: [http://apl.aip.org/about/about\\_the\\_journal](http://apl.aip.org/about/about_the_journal)

Top downloads: [http://apl.aip.org/features/most\\_downloaded](http://apl.aip.org/features/most_downloaded)

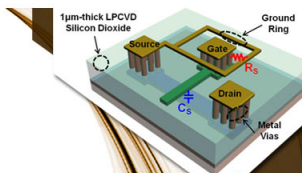
Information for Authors: <http://apl.aip.org/authors>

## ADVERTISEMENT



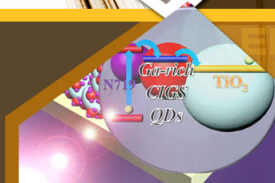
EXPLORE WHAT'S  
NEW IN APL

SUBMIT YOUR PAPER NOW!



### SURFACES AND INTERFACES

Focusing on physical, chemical, biological, structural, optical, magnetic and electrical properties of surfaces and interfaces, and more...



### ENERGY CONVERSION AND STORAGE

Focusing on all aspects of static and dynamic energy conversion, energy storage, photovoltaics, solar fuels, batteries, capacitors, thermoelectrics, and more...

## Optical properties of SrTiO<sub>3</sub> on silicon(100)

Yao Tian,<sup>1</sup> Carolina Adamo,<sup>2</sup> Darrell G. Schlom,<sup>2</sup> and Kenneth S. Burch<sup>1,a)</sup>

<sup>1</sup>Department of Physics & Institute of Optical Sciences, University of Toronto, Ontario M5S 1A7, Canada

<sup>2</sup>Department of Materials Science and Engineering, Cornell University, Ithaca, New York 14853, USA

(Received 19 August 2012; accepted 15 January 2013; published online 29 January 2013)

Epitaxial buffer layers enable the many functionalities found in perovskites to be integrated with silicon. However, epitaxial growth of SrTiO<sub>3</sub> on silicon is tricky and has so far only been achieved by molecular beam epitaxy. Nonetheless, previous investigations of these films were limited by the amorphous layer occurring at the interface. Through a combination of improved interface quality and an improved model, we report the optical properties of SrTiO<sub>3</sub> films on Si(100) investigated by spectroscopic ellipsometry. We find that the data are best described by a model with two different SrTiO<sub>3</sub> layers, potentially resulting from variations in the oxygen content. © 2013 American Institute of Physics. [<http://dx.doi.org/10.1063/1.4789752>]

SrTiO<sub>3</sub> is an important material for a wide range of applications, due to its unparalleled dielectric,<sup>1</sup> ferroelectric,<sup>2</sup> and piezoelectric properties.<sup>3</sup> The potential applications are limited, however, by the difficulty of integrating them with silicon technology. Towards this goal, it was recently demonstrated that the perovskite SrTiO<sub>3</sub> can be grown on Si(100) directly,<sup>4</sup> the most popular substrate in modern devices. Such integration can be used as a stepping stone to the integration of other perovskites with silicon, as SrTiO<sub>3</sub> serves as an excellent substrate for their growth. Indeed, this approach has been used to incorporate BaTiO<sub>3</sub>,<sup>5</sup> Pb(Zr,Ti)O<sub>3</sub>,<sup>6</sup> BiFeO<sub>3</sub>,<sup>7</sup> PbMg<sub>1/3</sub>Nb<sub>2/3</sub>O<sub>3</sub>-PbTiO<sub>3</sub>,<sup>8</sup> and other important perovskites with silicon.

When these films are sufficiently thin (5–6 unit cells thick), they are commensurately strained in biaxial compression resulting in robust ferroelectric behavior. The ferroelectricity in SrTiO<sub>3</sub>/Si (100) thin films is perhaps not surprising given the strong sensitivity of SrTiO<sub>3</sub> to strain<sup>9</sup> and chemical composition. This further suggests that the electronic and optical properties of SrTiO<sub>3</sub> films on Si (100) will be modified from their bulk values. Nonetheless, standard molecular beam epitaxy (MBE) techniques typically resulted in a complex interfacial layer. Thus, previous attempts to investigate the optical properties of SrTiO<sub>3</sub> films on Si were only able to determine the average response of the film. Since recent improvements in the growth of SrTiO<sub>3</sub> via MBE have enabled films with no interfacial SiO<sub>2</sub>, we have revisited the optical properties of these films. Through a combination of improved film quality and a model for analysis, we have determined the dielectric function of these SrTiO<sub>3</sub> films as well as the interfacial layer.

The optical properties were measured using a variable angle spectroscopic ellipsometer (VASE) with a rotating analyzer and an autocompensator from J.A. Woollam Co., Inc. The VASE instrument measures the ratio of  $\tilde{r}_p$  to  $\tilde{r}_s$  (the complex reflectance parallel and perpendicular to the plane of incidence). This ratio is typically expressed in terms of  $\Psi$  and  $\Delta$  defined as

$$\frac{\tilde{r}_p}{\tilde{r}_s} = \tan \Psi e^{i\Delta}. \quad (1)$$

For a bulk crystal, the Fresnel equations relate the ellipsometric parameters to the optical constants directly without any need for further analysis. However, for anisotropic crystals or layered materials there exists no analytical formula to directly extract the optical constants of the film from  $\Psi$  and  $\Delta$ . In this case, measurements are performed at multiple angles of incidence, then the data are fit to extract the optical constants. Nonetheless, by measuring  $\Psi$  and  $\Delta$  at various angles of incidence, one can determine the thickness and optical constants of constituent members of a multilayered material. Additionally, all the measurements can be done non-invasively and non-destructively.

The optical constants of the silicon substrate are sensitive to its doping level. Thus, we took data on a silicon substrate from the same batch. Knowing the optical constants of the substrate allowed us to precisely model the SrTiO<sub>3</sub>/Si system. The SrTiO<sub>3</sub> thin film was prepared by MBE via a kinetically controlled growth process. The native surface oxide of the silicon substrate was thermally removed *in situ* prior to film growth via a strontium-assisted deoxidation process. The details of the growth can be found elsewhere.<sup>4</sup> To prevent the interference from the substrate, the back surface of the silicon substrate is roughened intentionally.<sup>10</sup> Ellipsometric parameters of the SrTiO<sub>3</sub>/Si film were measured from 0.75 eV to 5.5 eV with 0.05 eV resolution, except in the range 2.4 to 4.6 eV where it was measured with 0.001 eV to properly capture the critical points of Si and SrTiO<sub>3</sub>. The measured  $\Psi$  and  $\Delta$  are shown in Fig. 1.

From Fig. 1, we can see there are several features in the experimental data. The feature around 1.4 eV results from interference. The peak at 3.4 eV is the natural result of the E<sub>1</sub> critical point of the silicon substrate.<sup>11</sup> There are also two small features around 3.7 eV and 4.7 eV. The former feature is due to the direct gap of the SrTiO<sub>3</sub> film and the latter one is due to the higher energy critical point of the SrTiO<sub>3</sub> film at 4.7 eV.

To properly extract the optical constants of SrTiO<sub>3</sub> as well as determine the homogeneity of the film, the dielectric function ( $\tilde{\epsilon}(E) = \epsilon_1(E) + i\epsilon_2(E)$ ) of the SrTiO<sub>3</sub> film is

<sup>a)</sup>Electronic mail: kburch@physics.utoronto.ca.

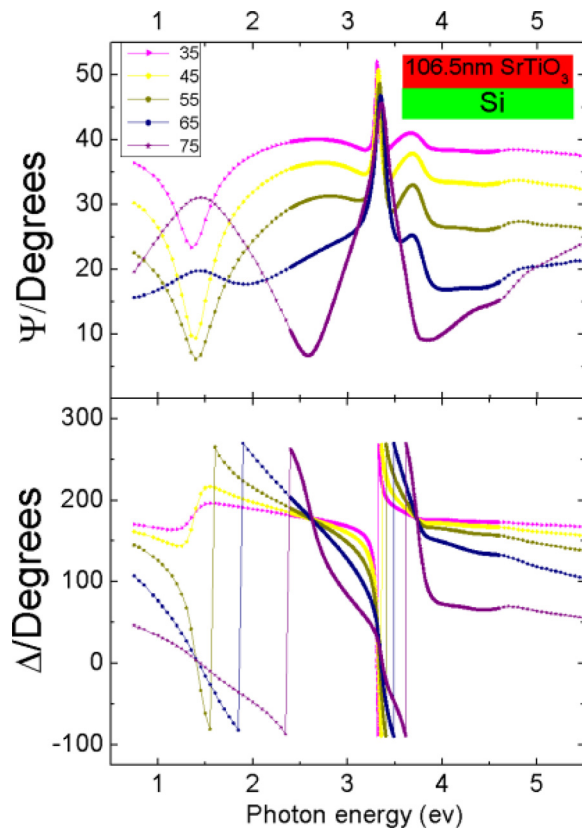


FIG. 1. Experimental data of  $\Psi$  and  $\Delta$  measured at various angle of incidence. Inset: Schematic view of the one layer model. Legend: Numbers indicate the angle of incidence.

defined using a sum of Tauc-Lorentz (TL) oscillators that are widely applied to interpret amorphous materials and thin films.<sup>12</sup> The imaginary part of the dielectric function in this model can be written as<sup>13</sup>

$$\epsilon_2(E) = \frac{A_L E_0 C (E - E_g)^2}{(E^2 - E_0^2)^2 + C^2 E^2} \Theta(E - E_g), \quad (2)$$

where  $E_0$  is the peak transition energy,  $A_L$  is the oscillator strength,  $E_g$  is the band gap,  $C$  is the broadening term, and  $\Theta$  is the step function. The real part is obtained from a Kramers-Kronig transformation. From the formula, we see that the sudden onset of absorption due to a band gap is included via a step function multiplied by a standard Lorentz oscillator. However, in the analysis of dielectric response of crystals, the parameters of each TL oscillator itself do not have a real physical meaning, but rather function to model the behavior of dielectric function phenomenologically. What is meaningful is the optical constants described by the sum of the TL oscillators.<sup>10,14</sup> Nonetheless, since the same approach was applied to all materials studied, relative trends between the materials are faithfully reproduced. First, we tried to fit the data with a one layer model including only a single layer of SrTiO<sub>3</sub> thin film on the silicon substrate (shown in the inset of Fig. 1). The difference ( $\delta\Psi = \Psi_{\text{measured}} - \Psi_{\text{fit}}$ ) between the measured ( $\Psi_{\text{measured}}$ ) and the fit ( $\Psi_{\text{fit}}$ ) with one SrTiO<sub>3</sub> layer is shown in Fig. 2. Similar results were seen in  $\delta\Delta$ . From Fig. 2 it is clear that the fit does not work well, especially in the region above the band gap of SrTiO<sub>3</sub> and at the  $E_1$  critical point of silicon. Various models were tried to account for the possible

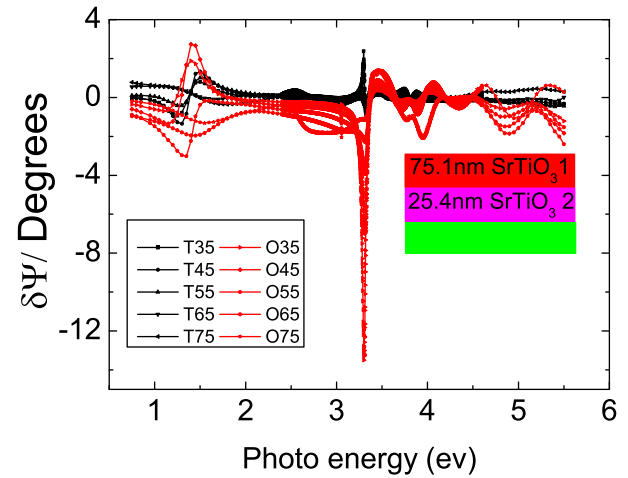


FIG. 2. Difference between measured  $\Psi$  and the fits of the two models. A significant improvement in the quality of the fit is obtained through the two-layer model, especially near the  $E_1$  critical point of silicon (3.4 eV). Legend: T and O indicate two-layer and one-layer model respectively. Numbers indicate the angle of incidence.

strain induced by the substrate and oxygen deficiency during the growth.<sup>15</sup> This included a graded model where the dielectric function varies continuously along the direction normal to the surface of the film. In addition, an effective medium layer between the SrTiO<sub>3</sub> layer and the silicon substrate was added to account for a mixture of SrTiO<sub>3</sub> and silicon.<sup>16</sup> However, these models did not substantially improve the fit. The failure of these models led us to try a less intuitive, though simpler model where there are two layers of SrTiO<sub>3</sub> in the film with different optical constants (shown in the inset of Fig. 2). The improved model resulted in a dramatic improvement of reduced chi-square ( $\chi^2/\nu$ , where  $\nu$  is the number of degrees of freedom) from 7.9 to 3.7. From Fig. 2, we can clearly see the dramatic reduction in  $\delta\Psi$  for the second model. This is especially true at the  $E_1$  critical point of the silicon substrate. The reason is a reduction in the absorption of the second layer of the SrTiO<sub>3</sub> films (see Fig. 3), which allows more light to reach the silicon substrate.

From the fit, the thickness of the top (second) layer is  $75.1 \pm 0.1$  nm ( $25.4 \pm 0.1$  nm), giving a total thickness of the SrTiO<sub>3</sub> film of  $100.5 \pm 0.2$  nm. This is in good agreement with the nominal thickness determined from *in-situ* RHEED during the MBE growth of the film.<sup>15</sup> We present the dielectric function of both layers in Fig. 3. Data for the second layer is only displayed below 3.76 eV since this is the energy where the penetration depth is smaller than the thickness of the top layer (see Fig. 4). As a comparison, the bulk SrTiO<sub>3</sub> is also measured with spectroscopic ellipsometry with resolution 0.05 eV from 0.75 eV to 5.5 eV. The optical constants of the bulk are also extracted by the sum of TL oscillators. A  $3.0 \pm 0.1$  nm-thick Bruggeman effective medium approximation layer was added to account for the surface roughness.<sup>17</sup> The extracted optical constants are in good agreement with the literatures<sup>17,18</sup> and plotted in Fig. 3 as well. From Fig. 3, we can see that the onsets of  $\epsilon_2(E)$  shift from the bulk value indicating the band gaps of both layers shift to lower energy. The reasons for the shifts will be discussed later.

In inset (c) of Fig. 3, we plot  $(\epsilon_2(E) \times E^2)^2$ , since in the vicinity of direct gap,  $\epsilon_2(E)$  has the energy dependence

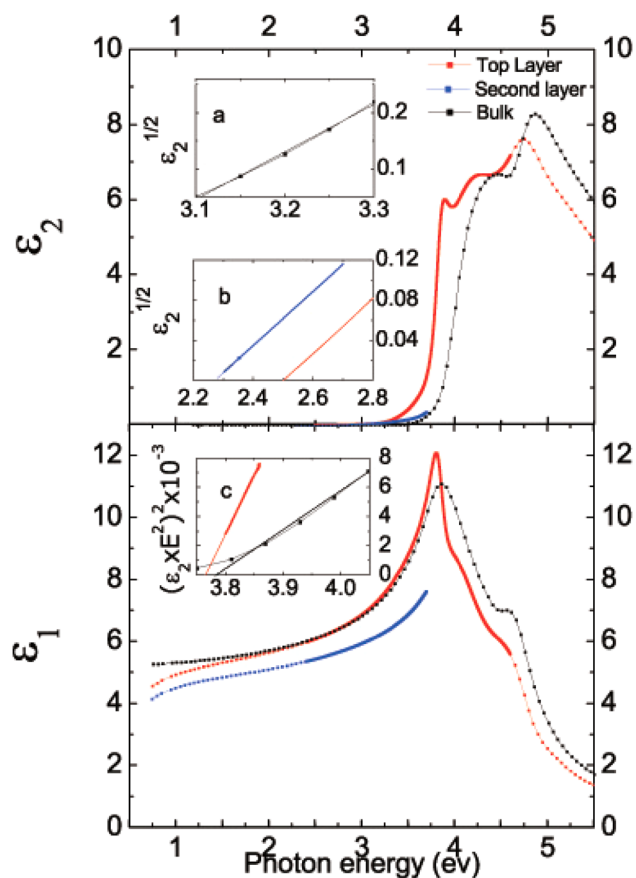


FIG. 3. Real and imaginary parts of the dielectric functions of the top layer SrTiO<sub>3</sub> (red), second layer SrTiO<sub>3</sub> (blue), and bulk SrTiO<sub>3</sub> (green). Inset: (a) Fit of the optical indirect band gap for the bulk. (b) Fits of the optical indirect band gaps for both top and second layers of SrTiO<sub>3</sub>. (c) Fits of the direct band gaps for top layer and bulk SrTiO<sub>3</sub>.

$(\epsilon_2(E) \propto (\frac{E}{E_g})^{-2} (\frac{E}{E_g} - 1)^{1/2})$ .<sup>19</sup> As expected, we observe a linear function of energy whose intercept gives a direct gap of  $3.77 \pm 0.03$  eV close to the bulk gap value of  $3.78 \pm 0.12$  eV determined by the same method. Since there is only limited data for the second layer, the direct gap cannot be determined. Also, at the edge of the indirect band gap,  $\epsilon_2(E)$  has the energy dependence given by  $\epsilon_2(E) \propto (E - E_g - E_p)^2$ , where  $E_p$  is the energy of phonon mode.<sup>19</sup> Thus, the optical indirect gap of both layers is determined by a linear fit between  $\epsilon_2(E)^{\frac{1}{2}}$

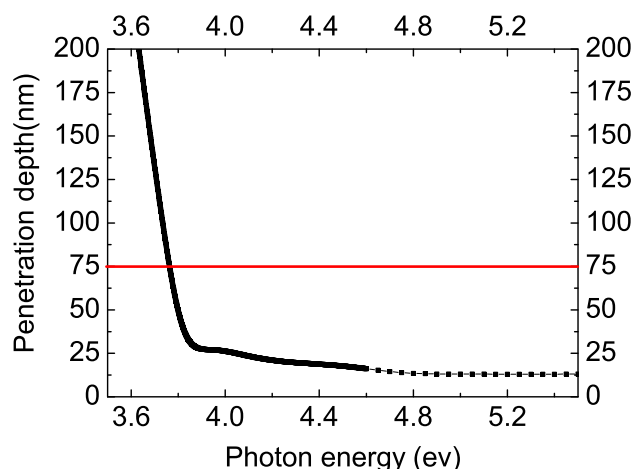


FIG. 4. Penetration depth of the top layer. The red line indicates the thickness of the top layer.

and the photon energy<sup>19</sup> (Inset (b) of Fig. 3). The results are  $2.51 \pm 0.01$  eV ( $2.28 \pm 0.01$  eV) for the top (second) layer, which are significantly lower than bulk value  $3.04 \pm 0.15$  eV (Inset (a) of Fig. 3) determined in the same manner.

According to band structure calculations of bulk SrTiO<sub>3</sub>,<sup>18,20</sup> the highest valence bands are formed by O 2p electrons and the lowest conduction bands are formed by Ti 3d electrons. The indirect gap is the transition between the  $\Gamma$  point and the R point and the direct gap occurs at the  $\Gamma$  point.<sup>18</sup> Reduction of the indirect gap has been reported in the literature and was attributed to the effects of strain<sup>21,22</sup> and oxygen deficiency.<sup>23,24</sup> In our case, it is hard to reach a firm conclusion for the reason for the reduced indirect gap. Commensurate growth on silicon corresponds to 1.7% compressive strain at room temperature.<sup>4</sup> In the tight bonding approximation, as the compressive strain reduces the lattice constants of SrTiO<sub>3</sub>, orbital overlap increases resulting in a reduction of the band gap. The reduction of the band gap due to the effect of strain has also been observed in SrTiO<sub>3</sub> thin films (14 nm) grown on LaAlO<sub>3</sub> (3% compressive strain).<sup>21</sup> Also, substrate induced strain could also cause optical anisotropy in the epitaxial film, which is not included in the two-layer model, so the structure obtained by the two-layer model may only be an approximation.

Nonetheless, we believe strain is not the cause of the two layers or reduction in the gap we observed. Specifically, it is hard to see how strain relaxation would result in two distinct layers rather than a gradual change. Furthermore, it has been shown that strain relaxation takes place quickly if the thickness of the SrTiO<sub>3</sub> film exceeds a critical value.<sup>25</sup> In particular, the strain is nearly fully relaxed in films of only 50 nm (whereas our films are 100 nm). Thus, strain is less likely to be the reason for reduction of the indirect band gap. Oxygen deficiency is more likely to be the cause of the two layers we observe. Indeed, it is well known that oxygen vacancies can act as shallow donors.<sup>26</sup> Kim *et al.* investigated the effect by optical absorption spectra on 100-nm-thick SrTiO<sub>3</sub> thin film deposited with different partial pressure of oxygen ( $P_{O_2}$ ).<sup>24</sup> They find anomalous absorption peaks below the optical band gap of bulk SrTiO<sub>3</sub> and the peak shifts to lower energy as  $P_{O_2}$  decreases. Based on a density-functional-theory (DFT) calculation, they argue that the effect should be due to Sr–O–O vacancy. Kan *et al.* found that the oxygen deficiency of SrTiO<sub>3</sub> caused by Ar<sup>+</sup> irradiation will induce luminescence at 2.8 eV below the gap.<sup>27</sup> The observation of a reduced indirect gap in these experiments is consistent with our results. Moreover, the deficiency of oxygen is also consistent with the film growth procedure.<sup>15</sup> The oxygen was turned off at the very beginning of the growth to prevent the formation of SiO<sub>2</sub>. Then, the oxygen was reintroduced later. Thus, the existence of the two layers is likely caused by the deficiency of oxygen.

In summary, spectroscopic ellipsometry has been performed on SrTiO<sub>3</sub> thin film grown on Si (100). The data are best described by a two layer model. The dielectric function of the second layer changes significantly from bulk. We ascribe this to the effect of oxygen deficiency at the beginning of growth.

Work at the University of Toronto was supported by NSERC, CFI, and ORF.

- <sup>1</sup>A. J. Moulson and J. M. Herbert, *Electroceramics*, 2nd ed. (John Wiley & Sons, West Sussex, 2003).
- <sup>2</sup>J. Li, J. Wang, M. Wuttig, R. Ramesh, N. Wang, B. Ruetter, A. P. Pyatakov, A. K. Zvezdin, and D. Viehland, *Appl. Phys. Lett.* **84**, 5261 (2004).
- <sup>3</sup>S.-E. Park and T. R. Shrout, *J. Appl. Phys.* **82**, 1804 (1997).
- <sup>4</sup>M. P. Warusawithana, C. Cen, C. R. Slesman, J. C. Woicik, Y. Li, L. F. Kourkoutis, J. A. Klug, H. Li, P. Ryan, L.-P. Wang *et al.*, *Science* **324**, 367 (2009).
- <sup>5</sup>V. Vaithyanathan, J. Lettieri, W. Tian, A. Sharan, A. Vasudevarao, Y. L. Li, A. Kochhar, H. Ma, J. Levy, P. Zschack *et al.*, *J. Appl. Phys.* **100**, 024108 (2006).
- <sup>6</sup>B. T. Liu, K. Maki, Y. So, V. Nagarajan, R. Ramesh, J. Lettieri, J. H. Haeni, D. G. Schlom, W. Tian, X. Q. Pan *et al.*, *Appl. Phys. Lett.* **80**, 4801 (2002).
- <sup>7</sup>H. W. Jang, S. H. Baek, D. Ortiz, C. M. Folkman, R. R. Das, Y. H. Chu, P. Shafer, J. X. Zhang, S. Choudhury, V. Vaithyanathan *et al.*, *Phys. Rev. Lett.* **101**, 107602 (2008).
- <sup>8</sup>S. H. Baek, J. Park, D. M. Kim, V. A. Aksyuk, R. R. Das, S. D. Bu, D. A. Felker, J. Lettieri, V. Vaithyanathan, S. S. N. Bharadwaja *et al.*, *Science* **334**, 958 (2011).
- <sup>9</sup>N. A. Pertsev, A. K. Tagantsev, and N. Setter, *Phys. Rev. B* **61**, R825 (2000).
- <sup>10</sup>K. S. Burch, J. Stephens, R. K. Kawakami, D. D. Awschalom, and D. N. Basov, *Phys. Rev. B* **70**, 205208 (2004).
- <sup>11</sup>P. Lautenschlager, M. Garriga, L. Vina, and M. Cardona, *Phys. Rev. B* **36**, 4821 (1987).
- <sup>12</sup>B. von Blanckenhagen, D. Tsonova, and J. Ullmann, *Appl. Opt.* **41**, 3137 (2002).
- <sup>13</sup>G. E. Jellison and F. A. Modine, *Appl. Phys. Lett.* **69**, 371 (1996).
- <sup>14</sup>A. B. Kuzmenko, *Rev. Sci. Instrum.* **76**, 083108 (2005).
- <sup>15</sup>D. G. Schlom and K. S. Burch, Private communication (2010).
- <sup>16</sup>T. H. Ghong, T. J. Kim, Y. D. Kim, and D. E. Aspnes, *Appl. Phys. Lett.* **85**, 946 (2004).
- <sup>17</sup>G. E. Jellison, Jr., L. A. Boatner, D. H. Lowndes, R. A. McKee, and M. Godbole, *Appl. Opt.* **33**, 6053 (1994).
- <sup>18</sup>S. Zollner, A. A. Demkov, R. Liu, P. L. Fejes, R. B. Gregory, P. Alluri, J. A. Curless, Z. Yu, J. Ramdani, R. Droopad *et al.*, *J. Vac. Sci. Technol. B* **18**, 2242 (2000).
- <sup>19</sup>P. Y. Yu and M. Cardona, *Fundamentals of Semiconductors: Physics and Materials Properties*, 3rd ed. (Springer-Verlag, Berlin, New York, 2001).
- <sup>20</sup>K. van Benthem, R. H. French, and C. Elsasser, *J. Appl. Phys.* **90**, 6156 (2001).
- <sup>21</sup>M. Tyunina, J. Narkilahti, J. Levoska, D. Chvostova, A. Dejneka, V. Trepakov, and V. Zelezny, *J. Phys.: Condens. Matter* **21**, 232203 (2009).
- <sup>22</sup>A. Dejneka, M. Tyuninab, J. Narkilahti, J. Levoska, D. Chvostovaa, L. Jastrabika, and V. A. Trepakova, *Phys. Solid State* **52**, 2082 (2010).
- <sup>23</sup>D. Ricci, G. Bano, G. Pacchioni, and F. Illas, *Phys. Rev. B* **68**, 224105 (2003).
- <sup>24</sup>Y. S. Kim, J. Kim, S. J. Moon, W. S. Choi, Y. J. Chang, J.-G. Yoon, J. Yu, J.-S. Chung, and T. W. Noh, *Appl. Phys. Lett.* **94**, 202906 (2009).
- <sup>25</sup>L. S.-J. Peng, X. X. Xi, B. H. Moockly, and S. P. Alpay, *Appl. Phys. Lett.* **83**, 4592 (2003).
- <sup>26</sup>N. Shanthi and D. D. Sarma, *Phys. Rev. B* **57**, 2153 (1998).
- <sup>27</sup>D. Kan, T. Terashima, R. Kanda, A. Masuno, K. Tanaka, S. Chu, H. Kan, A. Ishizumi, Y. Kanemitsu, Y. Shimakawa *et al.*, *Nature Mater.* **4**, 816 (2005).